Greener Journal of Geology and Earth Sciences
ISSN: 2354-2268
Vol. 5(1), pp. 28-51, 2023

http://gjournals.org/GJGES

Characterization of the Volcano-Seismic Activity around Nyiragongo Volcano and Location of its Crater by Means of Unified Scale

Mukange Besa Anscaire[1], Ntedika Mananga Ephraim[1], Zana Ndotoni André[1], Tondozi Kento Franck [1, 2]

[1]Mention Physics, Faculty of Sciences and Technology, University of Kinshasa, Kinshasa, DR Congo.
[2]Departement of internal Geophysics, Center of Research in Geophysic (CRG), Kinshasa, DR Congo.

ARTICLE INFO

Article No.: *120423152*
***Type*:** *Research*
Ful Text: *PDF, PHP, HTML, EPUB, MP3*

Accepted: *06/12/2023*
Published: *30/12/2023*

***Corresponding Author**
Prof. Mukange Besa Anscaire
E-mail: *anscairbesa@ yahoo.fr*

Keywords: *volcano-seismic activity, DRC-Virunga, Nyiragongo volcano, characterization scale, grid-areas, modules, structure factor, seismic species, geo-seismic signature, volume density*

ABSTRACT

Previous work consisted in characterizing some seismic zones, these include:

- The DRC area (10°E-35°E; 6°N-14°S), homogeneous, but once subdivided into square sub-zones of side 5°, was made heterogeneous but homogeneous in the Virunga region (25°E-30°E; 1°N-4°S°), (Mukange,2021b),
- The previously homogeneous Virunga area, subdivided into square sub-areas of dimension 1°, was made heterogeneous but homogeneous in the area around Nyiragongo volcano (29.00°E-29.50°E; 1.45°S-1.75°S) (Mukange, 2023c).

These characterizations were made possible by the design of a model by means of unified scale that generates seismic species.

The objective of this work is to characterize the "homogeneous" region around the Nyiragongo volcano, subdividing it into square sub-zones of dimension 0.1° and to find a technique for locating the crater. To do this, we designed a unified scale appropriate for characterization on the one hand, and on the other hand made the following assumptions:

- The crater is located at the place where the density volume of the number of volcanic earthquakes is abnormally high,
- The crater is located at the place where density volume of the energy of tectonic or volcano-tectonic earthquakes is very low.

The outcome of the research, following the processing of earthquake data from the area for a period from 2016 to 2021, revealed the following:

- The seismic species identified in this area are Iab, Iac, Ibb, Ibc, IIIbb and IIIbc, as structural factors, and (ab,ac,bb, and bc). The area's final degree of heterogeneity is 88%, with a 12% degree of homogeneity. As a result, the notion of a structure's homogeneity is dependent on the scale used to observe it.
- Hypotheses are confirmed. Indeed, according to our hypotheses and field observations, the crater is located at [29.25°E; 1.50°S].
- Other significant outcomes include:
- The number of earthquakes curve and the d-value have a good correlation (which characterizes the structure of the ground). It has been determined and confirmed that in this area, The seismic activity is completely dependent on the soil structure.

These findings support previous research (Mukange,2016), which found that the seismicity of DR C is better described (diversified) in terms of longitude (West to East) than latitude (North to South). Moving from west to east, the shape of the structure is the same for the DRC and Virunga; they are the inverse of Nyiragongo. Moving north to south, all three structures exhibit the same trend: seismic activity decreases from North to South.

1. INTRODUCTION

Our previous research (Mukange, 2016; Mukange 2021a-b) on the characterization of seismicity in an area in general, and that of the Democratic Republic of Congo (DRC) in particular, has highlighted, on a regional study scale, the homogeneity of seismicity in the Virunga area, which is home to Nyamulagira and Nyiragongo volcanoes. These two volcanoes are of great scientific interest and deserve to be thoroughly studied in order to improve monitoring and develop techniques and models for possible prediction. As a result, our characterization of Nyiragongo volcano's surroundings will consist of the following:

- Establishing the relationship between soil structure and seismic activity in the area. (modeling),
- To demonstrate that, upon closer examination, this previously revealed homogeneous seismic activity has a degree of heterogeneity.
- To attempt to locate the volcano's crater based on the following assumptions:
- The crater is situated in an area with a high density (volume) of earthquakes.
- The crater is found in areas with a low density (volume) of energy released by tectonic or volcano-tectonic earthquakes.

The crater is situated in an area where the density of earthquakes and energy released is low.

The East African Rifts system is presented as a continental extension of the global system of lithospheric fractures that snake through the middle of the Atlantic and Indian Oceans and extend into the Eastern part of Africa via the Gulf of Aden and the Red Sea (Mukange, 2016; Boden et al. 1988; Bantidi, 2014a). This fracture system is divided into two branches:

- The Eastern branch, which runs from the Afar triangle through Ethiopia and Kenya to the Tanzanian divergence in the north (Figure 1).

- The Western branch consists of a system of fractures that cross the Great Lakes garland, i.e., from Lake Albert (617 m) through Lake Edward (912 m), Lake Kivu (1462 m), Lake Tanganyika (780 m), Lake Rukwa (782 m), and Lake Malawi (460 m), and continues South to Mount Beira in Mozambique and southwest to Lake Kariba in Zimbabwe (Fig. 1). This branch thus covers most of the Eastern provinces of the DRC from latitude 4°N to latitude 8°S. From the Red Sea to the Zambezi, the East African Rifts are more than 6,000 km long and 40 to 60 km wide. The two branches split in two at the Aswan Lineament and join at Lake Malawi (Figure 1).The two branches are active (Bantidi et al.,2014b ; Mukange et al.,2013 ;Wafula 1999,2009,2011a,2011b ; Zana,1977,1981).

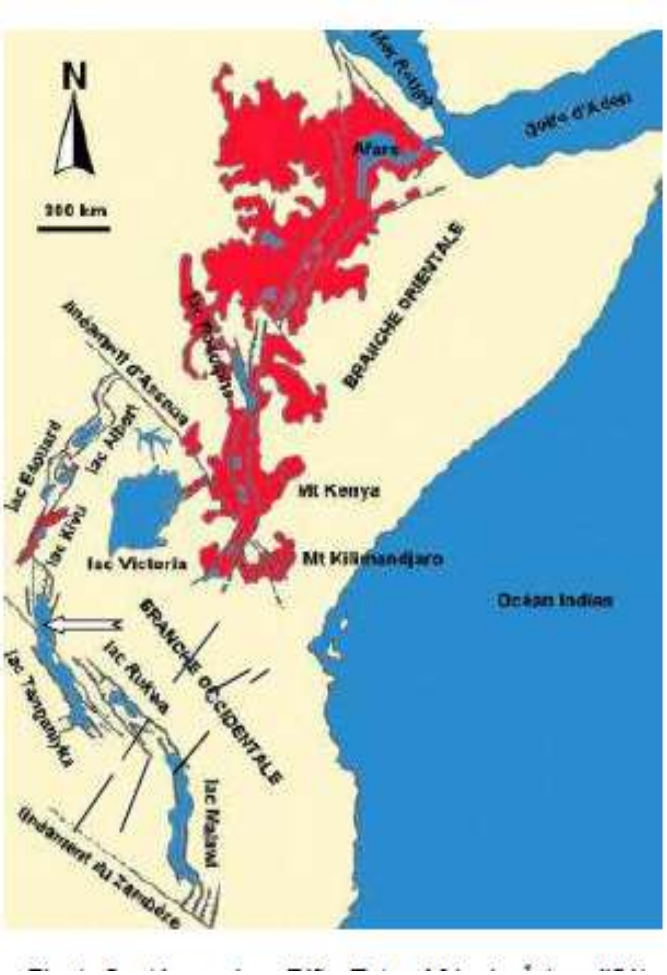

Figure 1: The East African Rift System is depicted with major faults as solid lines, water as blue, and volcanoes as red.

The Congolese Rift has three main volcanic provinces: Toro-Ankole province in the north, Virunga province (Nyiragongo and Nyamulagira volcanoes...) in the center, and South Kivu province in the south (Zana and Tanaka, 1981; Zana, 1982; Ngindu, 2009). (Wafula et al., 1989; Wafula et al., 2009).

The Virunga volcanic area is located in the far northwestern corner of Lake Kivu. This area is made up of eight volcanoes that are divided into three groups known as volcanic provinces: the eastern group, which includes Muhavura volcanoes (4127 m a.s.l.), Gahinga (3474 m), and Sabinyo (3647 m), the central group, which includes volcanoes Isoke (3911 m), Karisimbi (4506 m), and Mikeno (4437 m), and the western group (3056 m). Except for the brief eruption of Mugogo on August 1, 1957, volcanoes of the first two subgroups are currently dormant. Mugogo is 2350 meters above sea level and 11 kilometers north of Visoke; it is considered a satellite cone of the latter (Visoke).

Geophysical research carried out on the Virunga region in general and the Nyiragongo volcano in particular whose name means in English " the one that smokes" (Lubemba,2021),indicate that it is characterized by a flow of melilitite and feldpathic lavas of a speed 60 km/h at a temperature of 1.100°C (Bahaya,2021; Kamate, 2018; Ongendangenda, 2020).

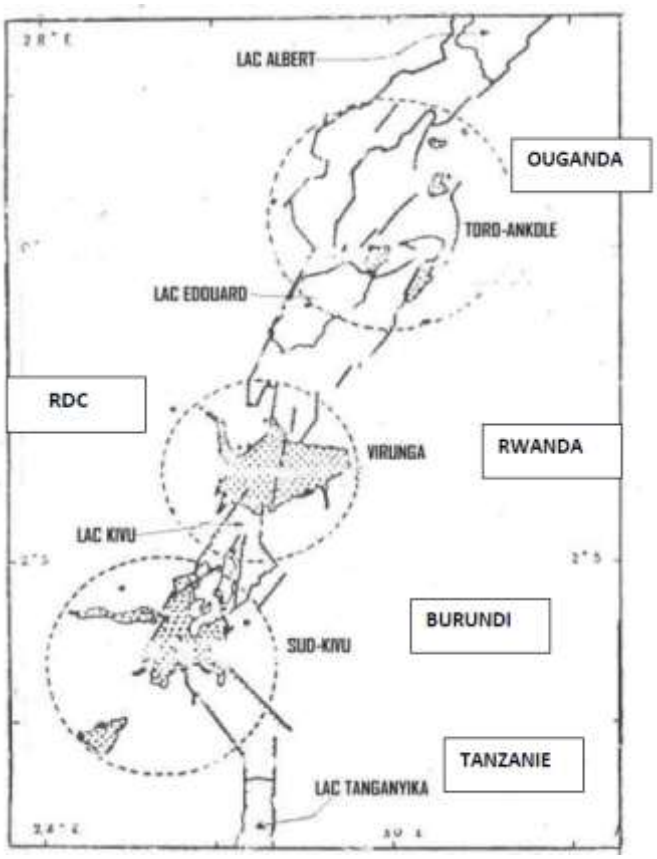

Figure 2 : The volcanic provinces of the Virunga region

The volcanoes of the western group are among the most active in the world today: Nyamulagira because of the frequency of eruptions (on average every two years) and Nyiragongo because of its permanent lava lake in the central crater. Note, in addition, that Nyiragongo is considered one of the most dangerous volcanoes on our planet due to its proximity to the city of Goma (15 km from the crater, with an estimated population of over one million) and the superfluidity of its lava, which can flow at speeds of up to more than 40 km/h (Wafula,2013). Both of these volcanoes lie within the same zone of the Rift Axis fractures (Figure 3).

Volcanic rocks of these two volcanoes are basalts rich in alkaline elements with a high potassium concentration; this would explain the lavas' hyperfluidity. The volcanic activity of these two volcanoes is of the Hawaiian type, with effusive and passive emission of lava with low viscosity (100-1000 poises) and very high temperature (1000°C). There are three other volcanoes of this type in the world: Mount Erebus in the Arctic, Kilauea in the Pacific, and Erta Alee in Ethiopia.

The classification based on seismogram frequencies is similar to that of the Redoubt volcano in Alaska: in the Virunga area, we record type A volcanic earthquakes (4-10 Hz), type B (1-4 Hz), type C (peak at 2.6 and 8 Hz), and tremors (1-2 Hz).

The last eruption of Nyiragongo volcano occurred on May 22, 2021.

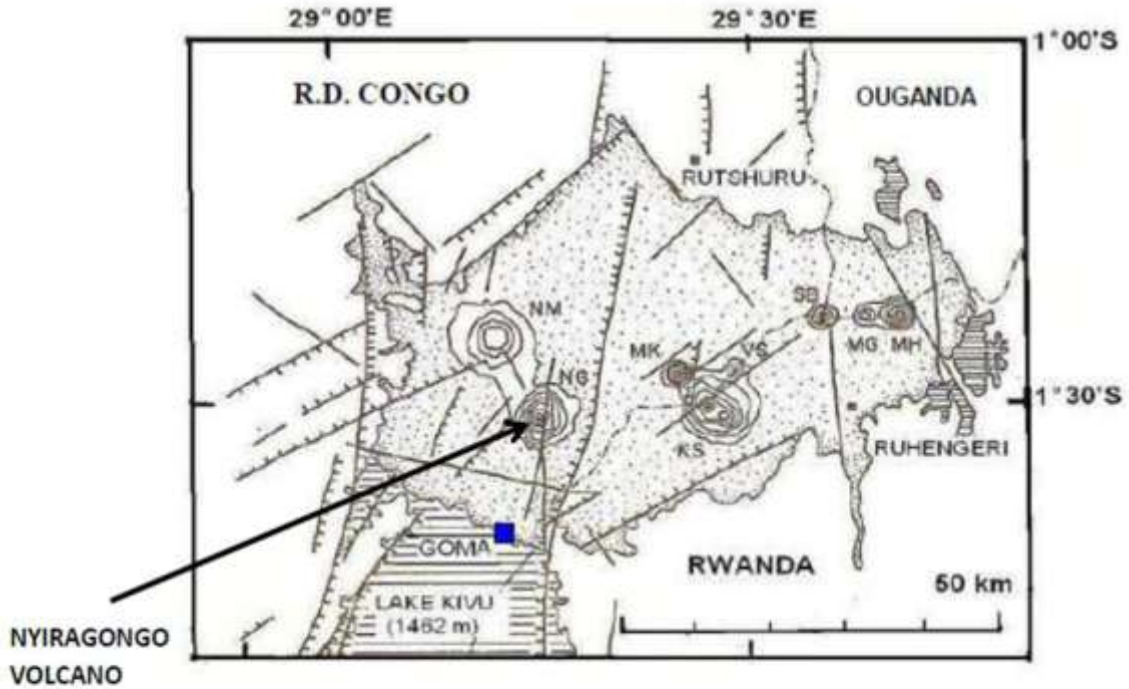

Extrait de la carte géologique de la région des Virunga.
Les lignes fermées : contour d'édifices volcaniques.
et : failles principales.
NM: volcan Nyamulagira; NG: volcan Nyiragongo; MK: volcan Mikeno;
KS: volcan Karisimbi; VS: volcan Visoke; SB : volcan Sabinyo;
MG :volcan Gahinga; MH : volcan Muhavura.

Figure 3: Structural geology of the Virunga region and location of volcanoes

More than 1300 volcanoes provide a rhythm to the earth's internal activity. The majority of them are active. The Nyiragongo volcano is a complex of three volcanoes aligned north-south: Baruta (3100 m) in the north, Nyiragongo main cone (99, 25°E, 1.50°S, 3470 m) in the center, and Shaheru (2800 m) in the south (Figure 4). Nyiragongo has the morphology of a stratovolcano (a volcano with an undulating shape and a stratified structure caused by the piling up of volcanic materials constituting the cone) (Simkin et al., 1981, cited by Wafula, 2013). Nyiragongo volcano is well-known for its lake, which was discovered in 1928. (Tazieff, 1977; Hamaguchi et al., 1982, cited by Wafula,2013).

Until 1977, the Nyiragongo crater was divided into three platforms: the first 180 meters from the crater's summit, the second 180 meters below the first, and the third 60 meters below the second. This lava lake's level fluctuated constantly, and by December 5, 1976, it had reached the critical level of the first platform (Pouclet, 1973, Tazieff, 1977, cited by Wafula, 2013).

Figure 4: Panorama of Nyiragongo volcano

2. METHOD OF DATA ANALYSIS

2.1. Data Analysis

The basic data for Nyiragongo volcano were collected at the Goma Volcanological Observatory (OVG) from 2016 to 2021 over the geographical area between 29°E and 29.5°E longitude and 1.45°S and 1.75°S latitude (Figure 5). The magnitudes, however, are missing from these data. To address the second hypothesis, we linked the tectonic earthquakes to their magnitudes as reported by the USGS.

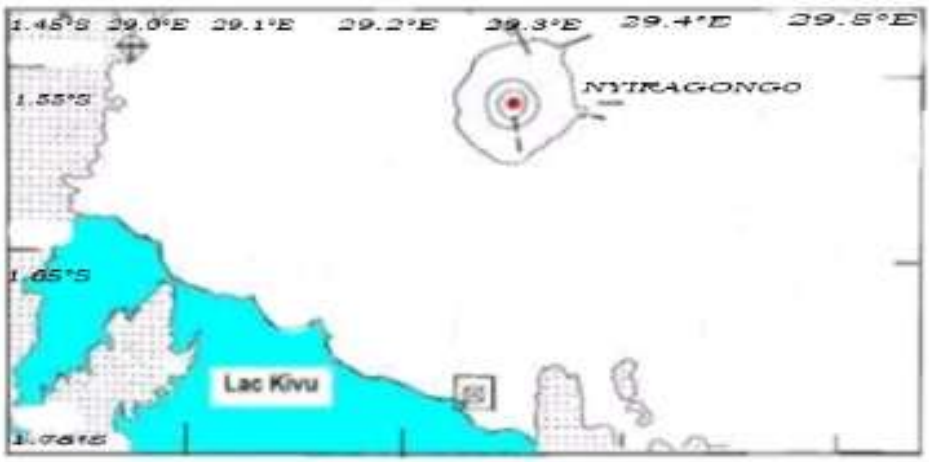

Figure 5: Precinct of the area being investigated

Fundamental data for each event contains the elements contained, for illustrative purposes, in the table below.

Table 1: Illustration of fundamental seismic data

Year	Month	day	Hour	Minute	Second	Latitude	Longitude	Depth(km)
2016	8	16	9	32	8,7	-1,447	29,181	4,1
2016	11	12	17	11	43,9	-1,447	29,218	5,6
2021	5	20	2	7	13,8	-1,448	28,565	17,1
2016	11	12	17	15	15,5	-1,449	29,204	23
2017	5	18	6	31	51,6	-1,453	29,104	30,8
2016	4	20	22	32	48,9	-1,453	29,156	41,5
2021	3	6	20	44	52,9	-1,457	29,327	52,7
2016	12	2	8	35	18,7	-1,462	29,267	66,9
2019	6	26	19	1	19,7	-1,464	29,27	70,4
2021	8	9	2	29	49,7	-1,465	29,173	79,8

The figure below depicts the findings of previous investigations (Mukange, 2021b) conducted in an area between 10° E-35° E longitude and 6° N-14° S latitude. The current study area (29.0°E-29.5°E and 1.45°S-1.75°S) falls within the "homogeneous" seismic area A42 (25°E-30°E and 4°S-9°S).

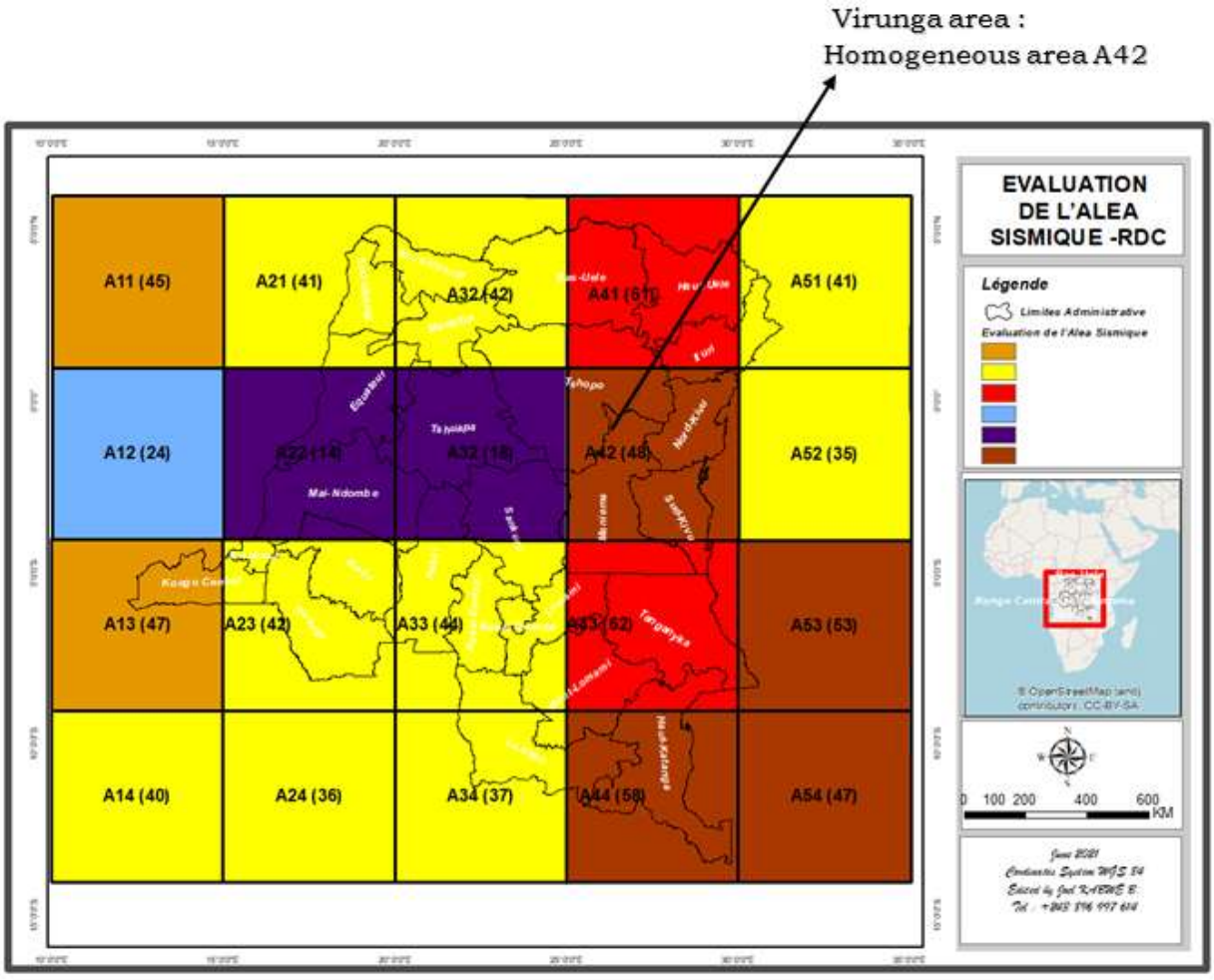

Figure 6: Seismic zoning in the Democratic Republic of Congo for seismic hazard assessment (Mukange, 2021b)

The results of the preceding figure have been transformed into curves (Figure 7), known as structure curves or "geoseismic signatures."

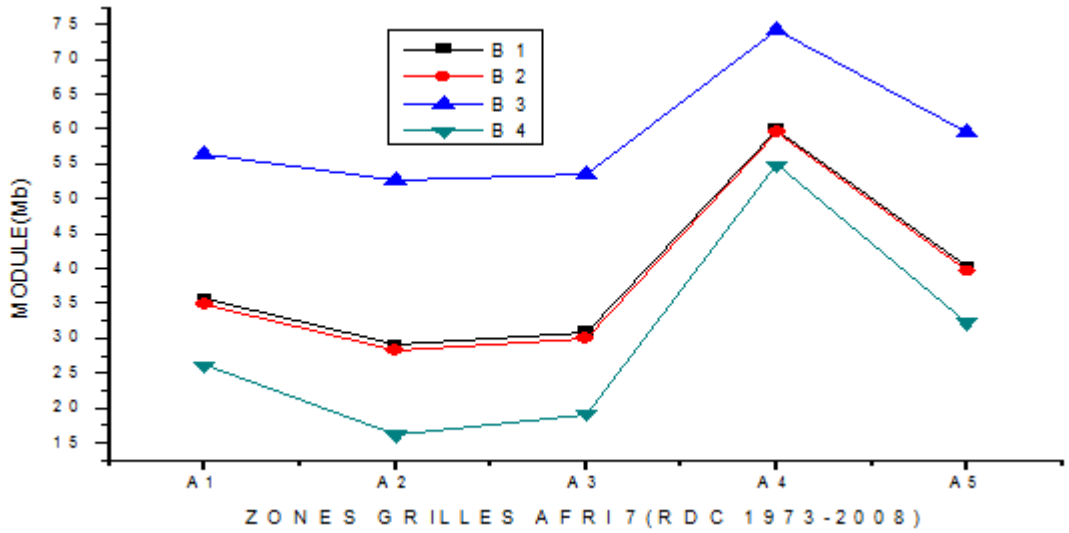

Figure 7: Seismic hazard curves in the DRC from Figure 6.

A more detailed study was conducted (Mukange, 2023a) highlighting the heterogeneity of the A42 zone (25-30°E, 1°N-4°S); it was sufficient to subdivide the said zone into square sub-areas of one degree side (Figure 8).

Figure (8) divides the area into two sections: the sub-area between 25° and 28°E and the sub-area between 28°E and 30°E. However, the first sub-area is divided into two parts, one between 25° and 26°E and the other between 26° and 28°E. A study similar to the previous ones will be conducted in this zone to characterize it and highlight its 'heterogeneous' nature.

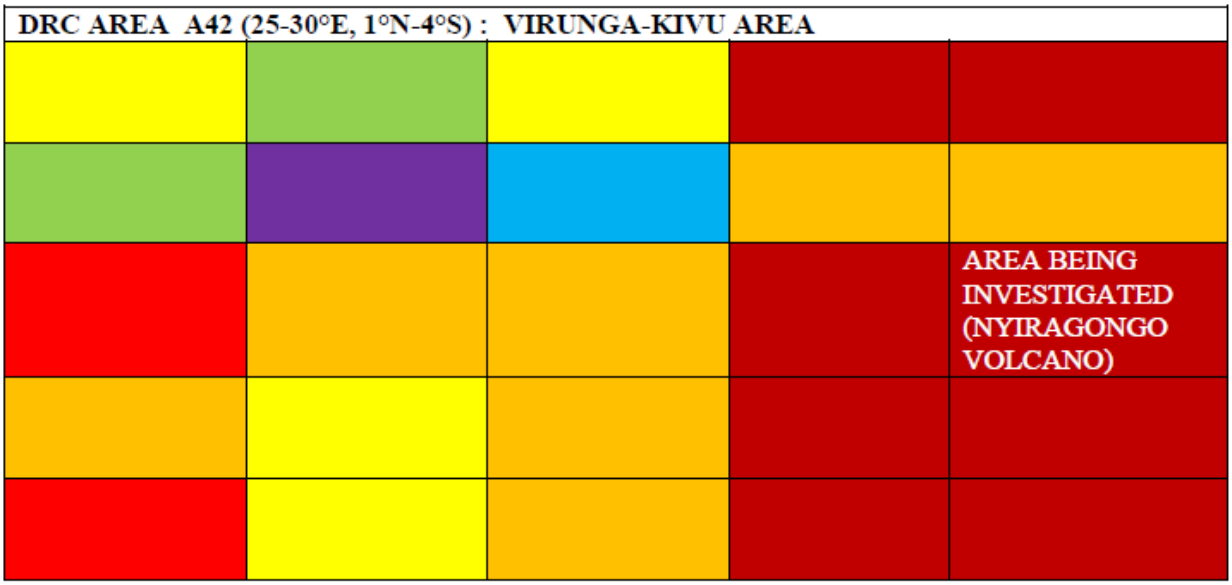

Figure 8: Seismic Zoning for Seismic Hazard Assessment in the Virunga area, A42

The geoseismic signature of figure (8) is represented by the figure bellow.

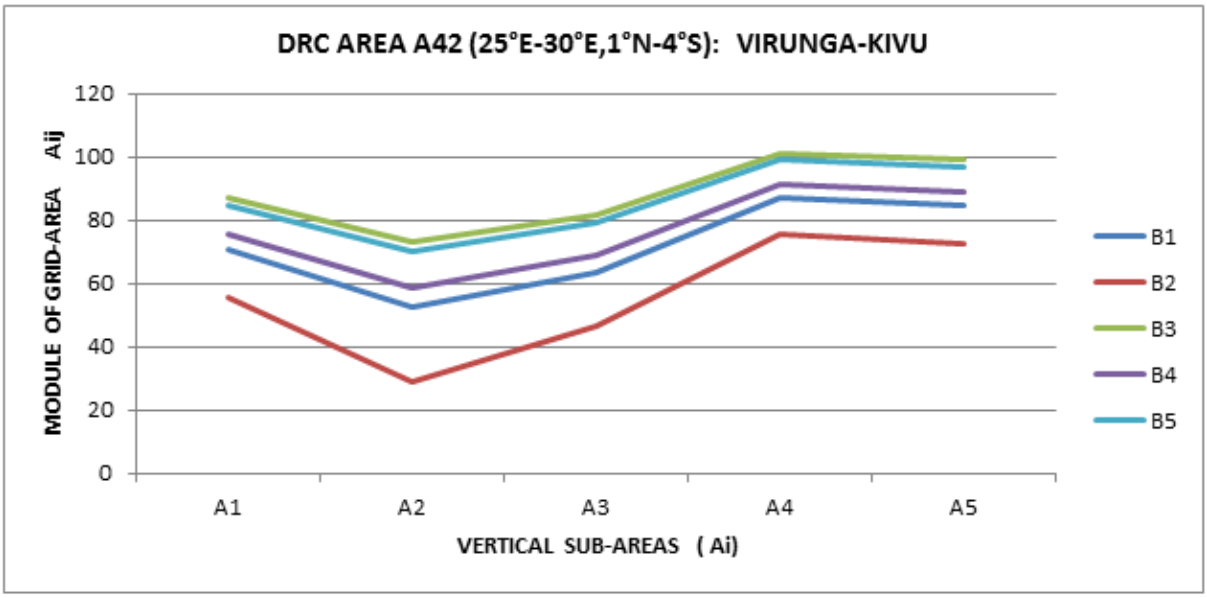

Figure 9: Transformation of the results of Figure 8 into curves

Figures (10-11) show the distribution of hypocenters around Nyiragongo volcano.

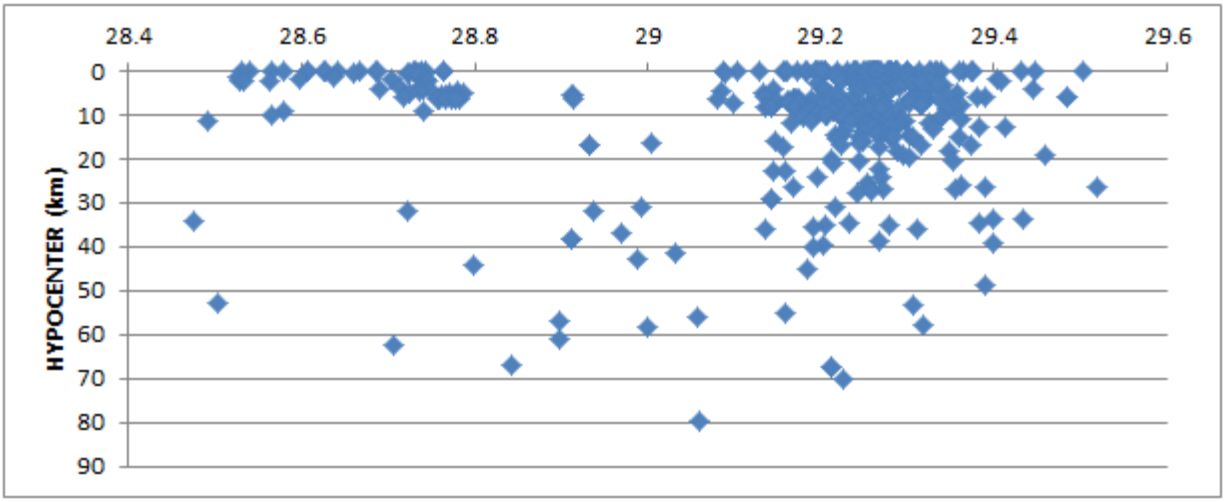

Figure 10: Distribution of hypocenters as a function of longitude around Nyiragongo volcano

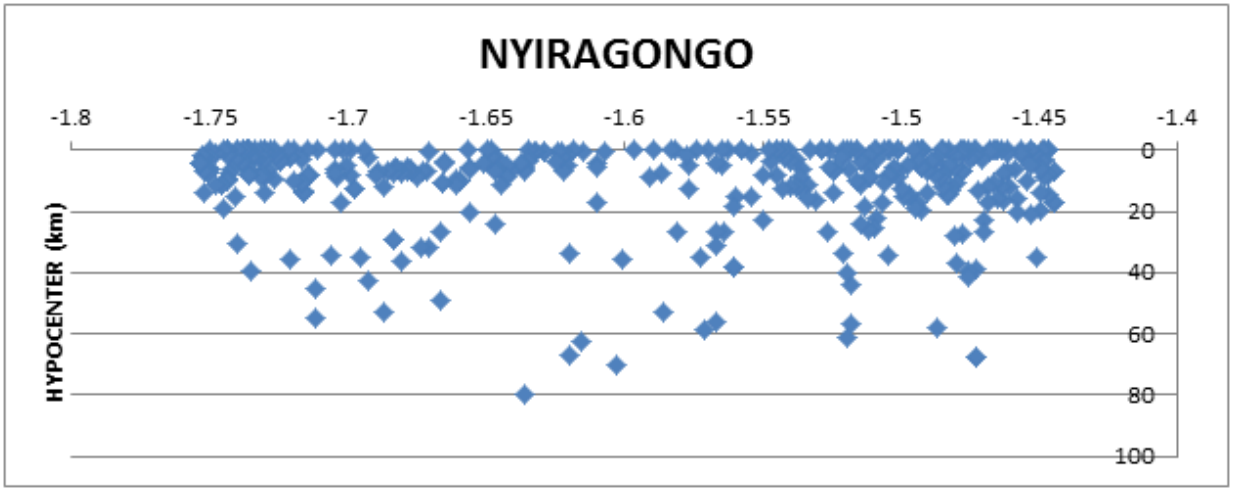

Figure 11: Distribution of hypocenters as a function of latitude around Nyiragongo volcano

2.2 Method of analysis

2.2.1. Introduction

Our main objective is to characterize the seismicity around the volcano. To do this, we must design a unified and appropriate scale. This scale must integrate various classical parameters that we will have to calculate in each sub-area; these are the following parameters:

- The total number of earthquakes,
- The total energy released by the earthquakes,
- The maximum Magnitude,
- The maximum depth of the hypocenters,
- Surface of each sub-area,
- Volume of each sub-area,
- Density of earthquakes,
- Density of energies,
- The b-value and the "d-value" Lay,1995; Mukange,2016),
- The degree of heterogeneity.

2.2.2. Method of analysis

The data will be processed by dividing the area into vertical (Ai) and horizontal (Bj) sub-areas of width 0.1° each, where we will calculate the above-mentioned parameters and group them in the table (5).

2.2.2.1. Vertical subdivision of the area

The study area is divided into five vertical sub-areas in 0.1 degree steps from west to east (Figure 12, Table 2).

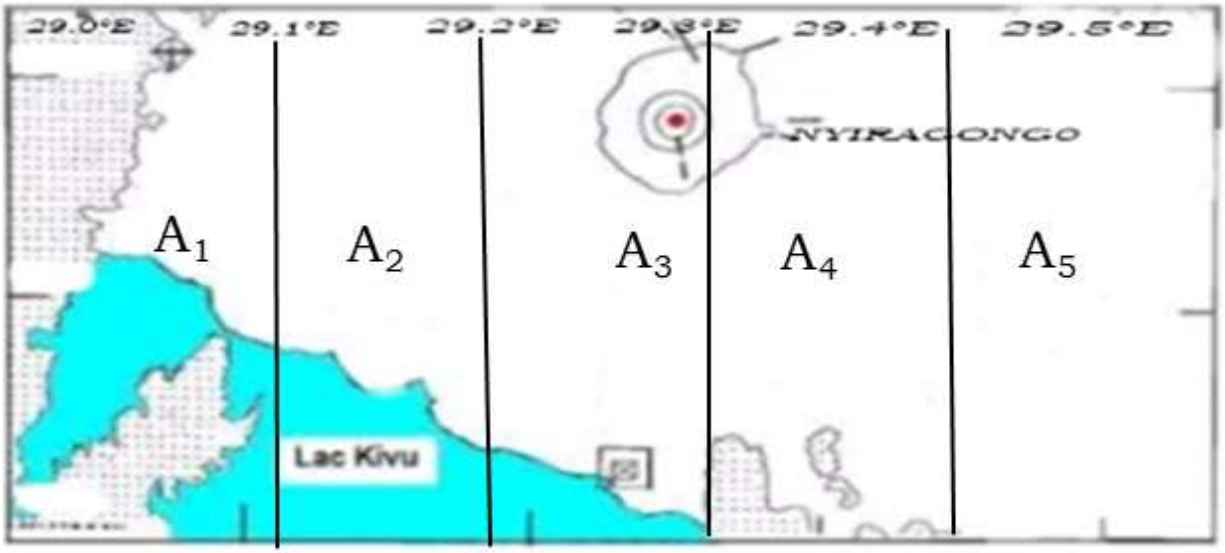

Figure 12: Subdivision of the area into vertical sub-areas (Ai)

Table 2: Limits and numbers of earthquakes in each vertical sub-area

N°	Areas	Limits of area		Number of earthquakes
		Longitude(°)	Latitude(°)	
1	A1	29°E-29,1°E	1,45°S-1,75°S	101
2	A2	29,1°E-29,2°E	1,45°S-1,75°S	114
3	A3	29,2°E-29,3°E	1,45°S-1,75°S	156
4	A4	29,3°E-29,4°E	1,45°S-1,75°S	30
5	A5	29,4°E-29,5°E	1,45°S-1,75°S	7
Total	A1+A2+A3+A4+A5	29,0°E-29,5°E	1,45°S-1,75°S	**408**

2.2.2.2. Horizontal subdivision of the area

The same area is, this time, subdivided into three horizontal sub-zones by steps of 0.1 degree. (Figure 13, Table 3).

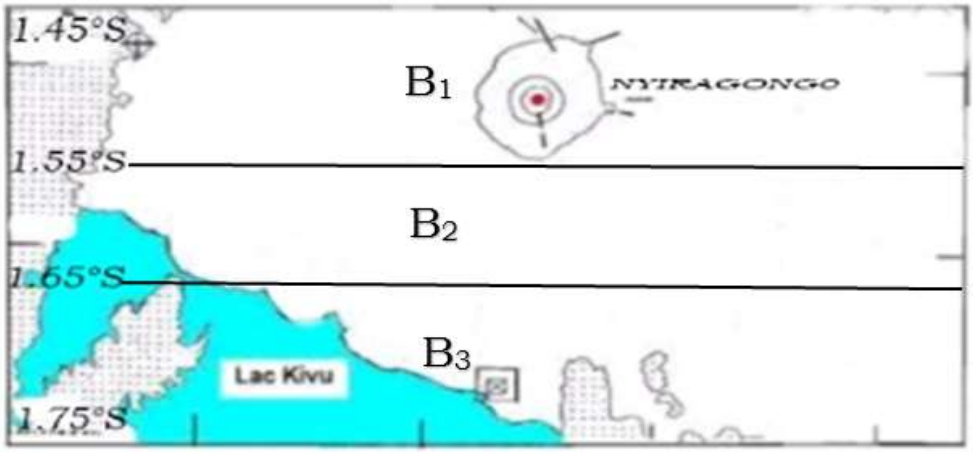

Figure 13: Subdivision of the area into horizontal sub-areas (Bj)

Table 3: Limits and number of earthquakes of each horizontal sub-area

N°	areas	Limits of the area		Number of earthquakes
		Longitude(°)	Latitude(°)	
1	B1	29,0°E-29,5°E	1,45°S-1,55°S	183
2	B2	29,0°E-29,5°E	1,55°S-1,65°S	72
3	B3	29,0°E-29,5°E	1,65°S-1,75°S	153
Total	B1+B2+B3	29,0°E-29,5°E	**1,45°S-1,75°S**	**408**

2.2.2.3. Calculation of seismic parameters

The classical seismic parameters for each sub-zone are calculated as follows:

2.2.2.3.1. The number of earthquakes

This consists of counting all the earthquakes that have occurred in each sub-area for the period from 2016 to 2021 (Tables 1-2).

These results are converted into percentages according to the following relationship:

$$N(j) = N_j.\frac{100}{N_k} \quad (1)$$

Where N_j is the total number of earthquakes in each Ai or Bj subarea. N_k is the total number of earthquakes in the whole study area.

2.2.2.3.2. The maximum magnitude

The operation consists in locating the largest magnitude recorded in each sub-area.

2.2.2.3.3. The energy of the earthquakes

The seismic energy released by each earthquake is determined, in Erg, through the formula

$$logE(Erg) = 5.8 + 2.4m_b \quad (2)$$

Thus, the total energy (E_Tk) in the sub-zone (k) is the sum of the energies of each event.

In percent, we use the following formula:

$$E(j) = E_j.\frac{100}{E_k} \quad (3)$$

With 〖 E〗_k, the total energy released by all recorded earthquakes in the entire study area.

2.2.2.3.4. The maximum and minimum depth

This identifies the greatest depth (hypocenter) recorded in each sub area.

2.2.2.3.5. The surface of each sub-area

Each sub-area has a rectangular shape whose surface (S) is calculated using the following formula:

$$S=L.l \quad (4)$$

With L and l, respectively the length and width of the subarea.

Recall that 1°=111.11km

2.2.2.3.6. The volume of each sub-area

The determination of the volume (V) of each sub-area is done using the formula below:

volume=area*maximum depth **(5)**

2.2.2.3.7. The volume density of earthquakes

The volume density (Ds) of earthquakes in each sub-area is obtained by the following formula:

$$\boldsymbol{D_s} = \frac{N_s}{V} \quad (6)$$

Ns is the total number of earthquakes in each sub-zone (Ai or Bj), (V) the volume of each sub-zone.
The volume density of earthquakes in percentage is determined by the following relation:

$$\boldsymbol{D_{(sl)}(\%) = \frac{D_s.100}{D_T}} \quad (7)$$

With $\boldsymbol{D_E = \frac{E}{V}}$

$\mathbf{D_T}$, $\mathbf{V_T}$, $\mathbf{N_T}$ represent respectively the total density, the total volume and the total number of earthquakes of the whole area constituted by the sub-areas Ai or Bi.

2.2.2.3.8. The volume density of energy

The volume density of energy in percentage is calculated in the same way as that of the earthquakes provided that the number of earthquakes in the zone or subzone is replaced by the energy. Hence:

$$\boldsymbol{D_E = \frac{E}{V}} \quad (8)$$

In percentage it is demined for each sub-area by the following relationship:

$$D_{(Ei)} = \frac{D_{(Ei).}}{D_{(Ek)}}.100 \quad (9)$$

2.2.2.3.9. The b-value and the d-value

The relationship
:

$$logE(Erg) = 5.8 + 2.4m_b \quad (10)$$

Used to characterize the seismic activity through the calculation of the value of the angular coefficient b, called the b-value (reference). This parameter has not attracted our attention.
In the same way as before,

The relationship:

$$\log(N) = a' + d.H \quad (11)$$

is used to characterize the soil structure through the calculation of the value of the angular coefficient d, introduced by us, called the d-value (Table 4, Figure 14).

Where ,m_b is replaced by H , the depth in relation.

Table 4: Statistics on the number of earthquakes by depth range

H≥	N	LOG(N)
0	114	2,00432
5	77	1,72428
10	39	1,41497
15	25	1,38021
20	19	1,36173
25	14	1,36173
30	14	1,27875
35	11	1,25527
40	9	1,17609
45	6	1,04139
50	5	0,95424
55	4	0,90309
60	4	0,8451
65	4	0,69897
70	2	0,30103
75	1	0

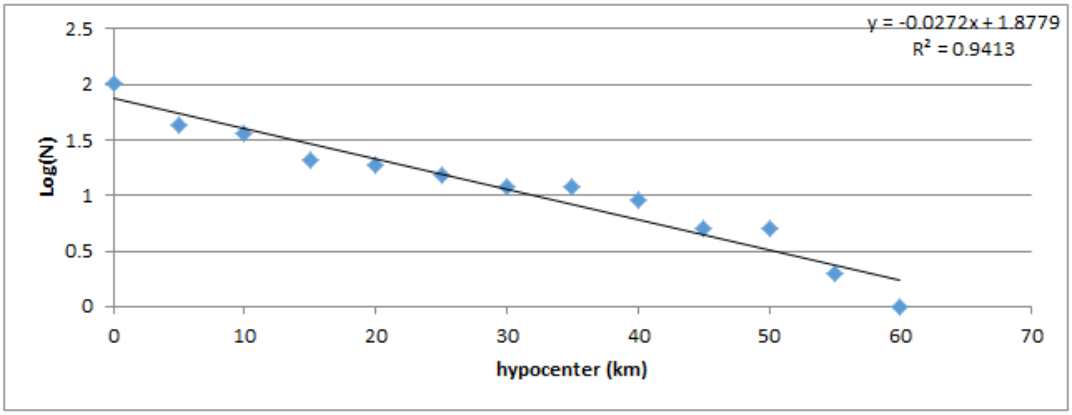

Figure 14: An illustration of how the parameter d-value is determined.

At the appropriate time, the parameter called "degree of heterogeneity" will be defined and calculated.

3. Presentation and discussion of findings

3.1. Presentation

The values of the various parameters calculated by using the above formulas are shown in the table below:

Table 5: **Synoptic table of calculated seismic parameters**

Areas	d-value	Number of earthquakes	Number (%)	Power (Erg)	power(%)	maxM	maxH (km)	sur face (km2)	Volu me (km3)	Density volume earthquakes	Volume density of power	Density of earthquakes (%)	Power density (%)
A1	0,0198	101	24,754902	7,86E+18	9,32E+01	5,2	79,8	363	28967,4	0,003	6,31E+13	106,389	93,257
A2	0,023	114	27,9411765	1,38E+17	1,64E+00	4,69	70,1	363	25446,3	0,00448	1,11E+12	136,700	1,637
A3	0,03	156	38,2352941	9,68E+15	1,15E-01	4,24	58,0	363	21054	0,00740	7,78E+10	226,088	0,114
A4	0,0225	30	7,35294118	2,91E+16	3,45E-01	4,44	48,8	363	17714,4	0,00169	2,34E+11	51,675	0,345
A5	0,031	7	1,71568627	3,85E+17	4,57E+00	4,91	26,6	363	9655,8	0,0007	3,09E+12	22,120	4,567
B1	0,0262	183	44,8529412	3,85E+17	4,57E+00	4,91	67,3	616	41456,8	0,0044	3,09E+12	134,692	4,567
B2	0,0179	72	17,6470588	1,23E+18	1,46E+01	4,91	79,8	616	49156,8	0,0014	9,88E+12	44,692	14,593
B3	0,0294	153	37,5	6,81E+18	8,08E+01	5,2	55,0	616	33880	0,0045	5,47E+13	137,795	80,799
TOUT	0,0297	408	100	8,43E+18	1,00E+02	5,2	79,8	1848	124494	0,00327	6,77E+13	100,000	100,020

3.2. DISCUSSION OF THE RESULTS

3.2.1. Design of the characterization scale

The characterization of the seismic activity of an area requires the design of a unified characterization scale that can reasonably incorporate all calculated parameters (Table 5). For our purposes, our characterization scale consists of three parameters and is written as follows:
X_12 , consisting of two parts, the form factor and the structure factor:

where
X is the volume density of energy (D_E in %) of each sub-zone. It is the "form factor".
X can take the value I, II, III or IV, with :

I, if D_E (%) ≤25% ;
II, if D_E25% < D_E (%) ≤ 50%,
III, if D_E (%) > 50%

The number 1 in subscript represents the earthquake volume density (D_s in %) of each subarea. It is defined as follows:

If D_s > 50% then the number 1 takes the index b otherwise the index a.
Number 2 is interested in the value of d-value and takes the following values:

if d-value is <0.01, then number 2 takes index a,
if 0.01≤ d-value ≤0.02, then number 2 takes index b,
if d-value is >0.02, then 2 takes index c.

The group, of numbers (1,2) in index is called "structure factor".

The combination of our three seismic parameters assigns to each sub-area a unique value called seismic species whose results are contained in Table (7).

3.2.2 Interpretation of the results

The interpretation of the results consists of characterizing the area and locating the crater of the volcano on the basis of the results obtained and hypotheses made.

3.2.2.1. Seismic species, seismic levels and color

The seismic species associated with each sub-area were ranked in ascending order corresponding to the level of seismic activity and ground structure. Finally, each seismic level is associated with a color (Tables 6-7).

Table 6: Color code associated with each seismic level. follows:

If D_s > 50% then the number 1 takes the index b otherwise the index a.

Number 2 is interested in the value of d-value and takes the following values:

if d-value is <0.01, then number 2 takes index a,
if 0.01≤ d-value ≤0.02, then number 2 takes index b,
if d-value is >0.02, then 2 takes index c.

The group, of numbers (1,2) in index is called "structure factor".
The combination of our three seismic parameters assigns to each sub-area a unique value called seismic species whose results are contained in Table (7).

Table 6: Color code for each seismic level.

Seismic level	colours
1	Pink
2	Blue
3	Green
4	Yellow
5	Purple
6	Orange
7	Light red
8	Dark red

Table 7: Color code, seismic species and seismic level associated with each sub-area.

Sub areas	**Seismic species**	**Seismic level** $(a_i)\ ou\ (b_j)$	**Colour code**
A1	IIIbb	6	orange
A2	Ibc	4	Yellow
A3	Ibc	4	Yellow
A4	Ibb	3	Light green
A5	Iac	2	Light blue
B1	Ibc	4	Yellow
B2	Iab	1	Pink
B3	IIIbc	7	Light red

This scale, in comparison to the previous one (MUKANGE 2021a), has some simple innovations for the sake of the cause: While containing several parameters,

- It has been greatly simplified to three parameters,

- It introduces and exploits the concept of volume density in particular (of power or of the number of earthquakes).

3.2.2.2. Vertical and horizontal zoning map

The results of table (7) lead to the creation of the seismic zoning maps shown below.

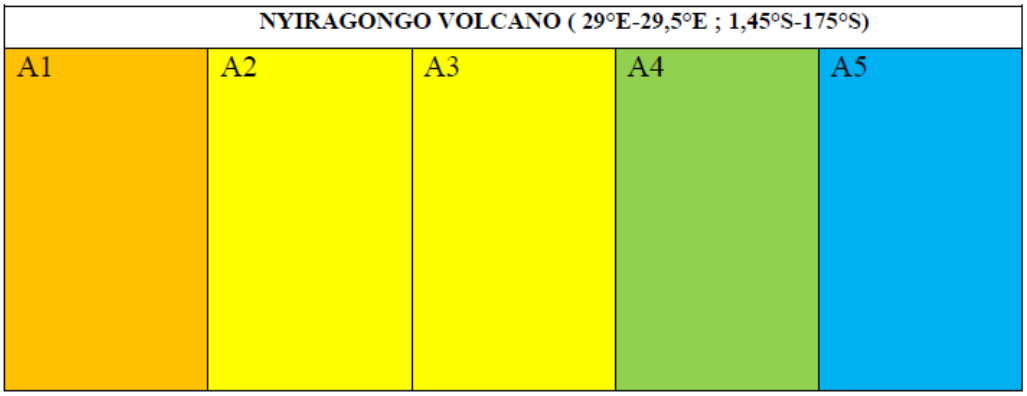

Figure 15: Seismic zoning map, vertical subdivision.

Sub-areas A 2 and A 3 have the same structure, as shown in the above map. A 1 has a complex structure.

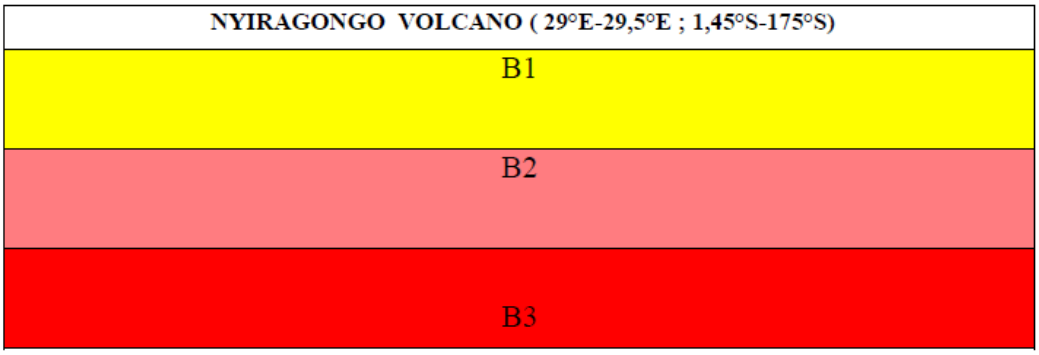

Figure 16: Seismic zoning map, horizontal subdivision.

We notice that each sub-area is distinct, and that when comparing the two subdivisions (Figure 15 and 16) on the eight sub-areas, only one color is shared (red). This demonstrates that seismicity and ground structure are not the same when studied vertically or horizontally.

3.2.2.3 Degree of heterogeneity

The degree of heterogeneity is determined by the ratio (in percentage) of the number of different colors to the total number of sub-areas (Table 8). It can also be calculated as the ratio of the distinct colors to the total number (8) of possible colors in the table (7).

Table 8 : shows the overall degree of heterogeneity of the sub-areas.

Sub-areas	Degree of hetérogeneity	Degree of heterogeneity in %
A_i	4/5	80 %
B_i	3/3	100 %
Average		90%

This area, which was previously homogeneous and subdivided into sub-areas, is no longer homogeneous: when studied vertically and horizontally, it exhibits a degree of heterogeneity of 80 and 100%, respectively, for a total of 90%.

3.2.2.4 Interpretation of other parameters

The evolution of the parameters according to sub-zones is shown below.

3.2.2.4.1 Evolution of the d-value

The d-value defines the soil structure, and its evolution by sub-area is as follows:

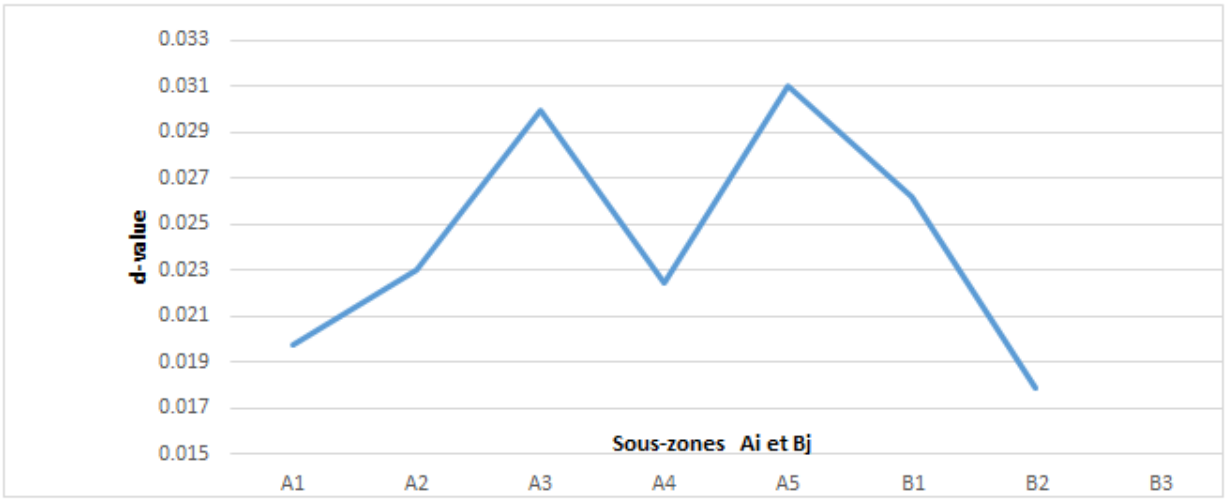

Figure 17 : depicts the evolution of the parameter d-value in each sub-area.

This curve demonstrates that the structure of sub-area A2 is similar to that of A4 and nearly identical to that of A3 and A5.

3.2.2.4.2 The evolution of Ai and Bj as a function of maximum depth

The characterization is carried out here by following the distribution of hypocenters on each horizontal sub-area.

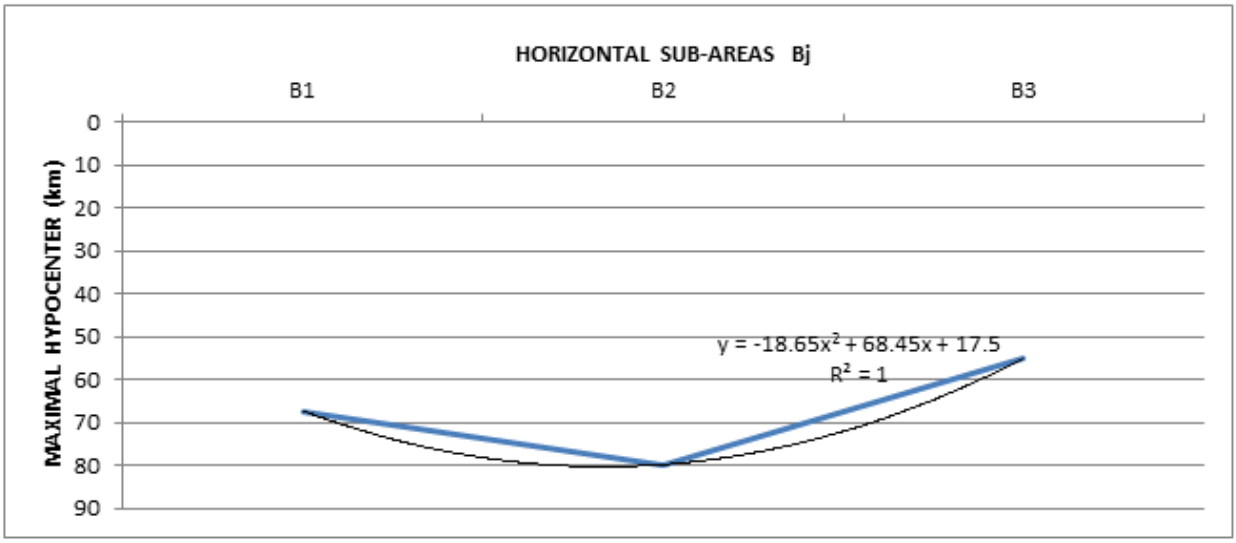

Figure 18: Distribution of maximum hypocenters in each Bj sub-area: modeling

We observe that the distribution of maximum hypocenters from north to south (Bj) around Nyiragongo volcano follows a parabolic law of upward concavity; The shape of the above curve is similar to that obtained in our previous research (Mukange,2021b).

Indeed, the curve below from the above research depicts the seismic activity (module on the ordinate) as a function of depth in Basaltic (Bi, on the abscissa) and sub-basaltic (SM1) layers in Virunga area, i.e., from 25 to 105 km in depth.

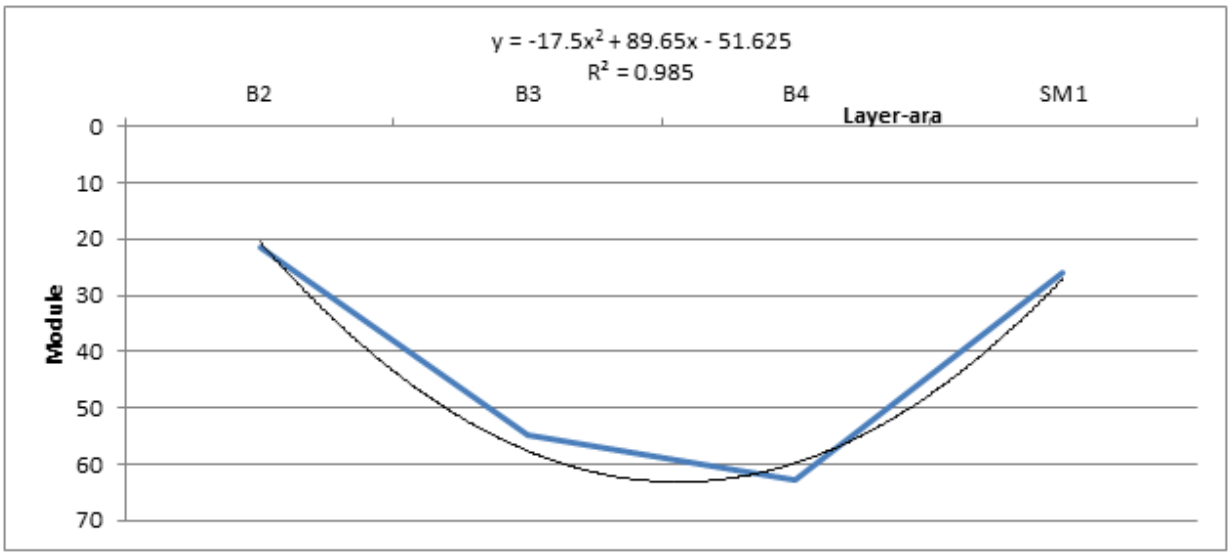

Figure 19: Seismic activity behavior in the basaltic and sub-Basaltic area of Virunga area

We conclude that the ground structure studied from North to South (horizontal subdivision) near Nyiragongo volcano is similar to that studied between 25 and 105 kilometers away in the Virunga region.

The characterization is carried out in this case by following the distribution of hypocenters on each vertical sub-area.

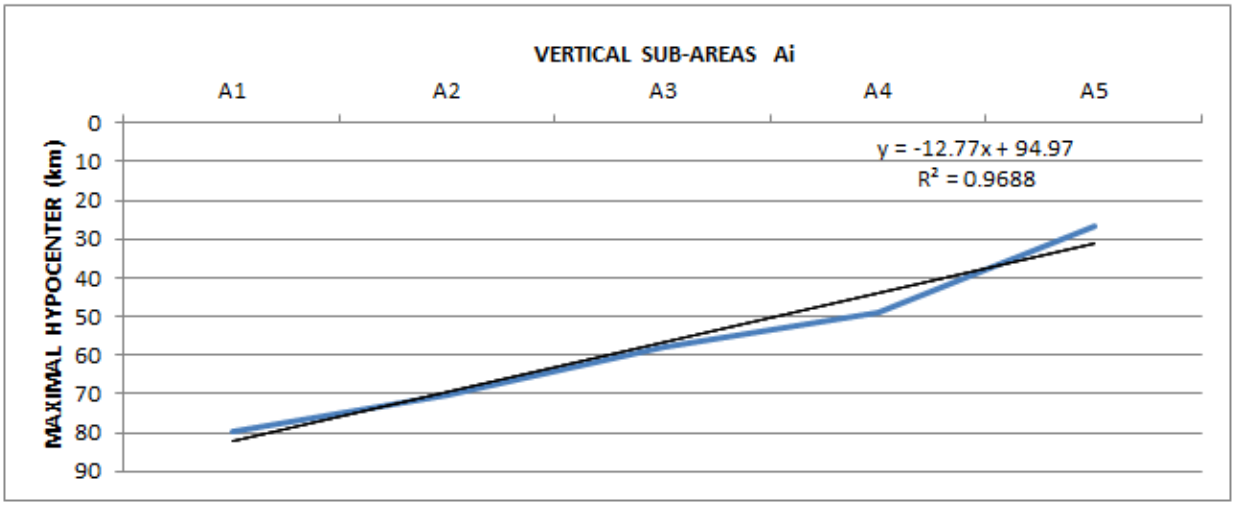

Figure 20: Distribution of maximum hypocenters in each sub-area AI (artificial intelligence): modeling Maximum depths decrease linearly from West to East.

We observe that the distribution of maximum hypocenters from North to South (Ai) around Nyiragongo volcano follows a linear increasing law; the shape of this line is similar to that obtained in our previous research (Mukange).

Indeed, the straight line below from the aforementioned study depicts seismic activity (module on the ordinate) as a function of depth in the granitic layer (Gi) in the Virunga region, i.e. from 0 to 20 km depth.

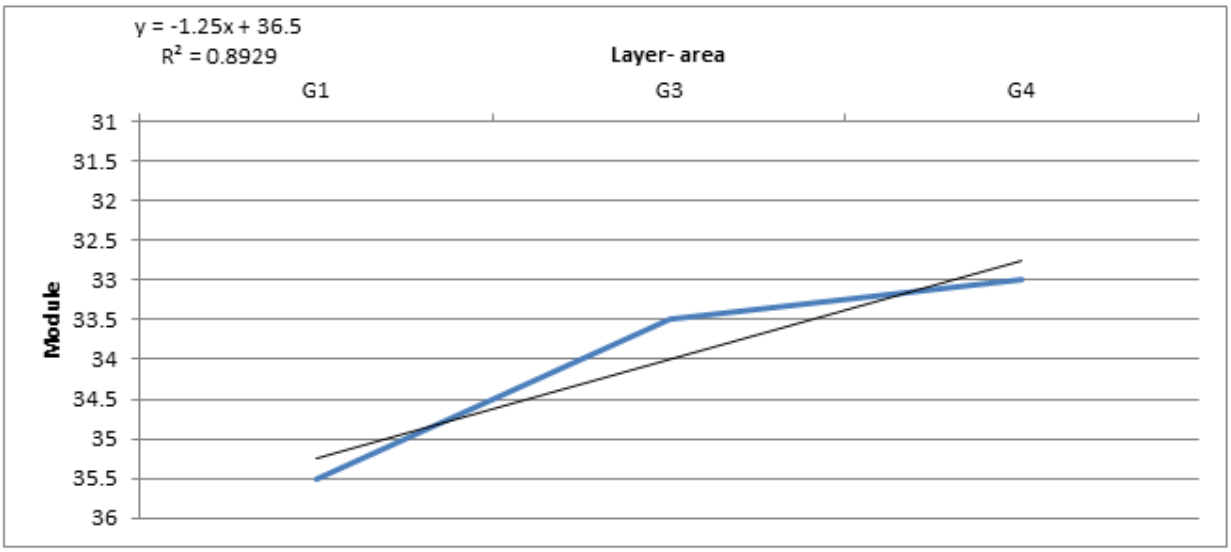

Figure 21: Seismic activity behavior in the granitic area of the Virunga area

We conclude that the ground structure studied using vertical subdivision (Ai) in the vicinity of Nyiragongo volcano is similar to that studied in the granitic area of the Virunga area.

3.2.2.4.3 Comparison of soil structure and seismic activity

Figures 22 and 23 depict the seismic activity and soil structure in Virunga area, respectively, by using angular coefficients (b-value and d-value).

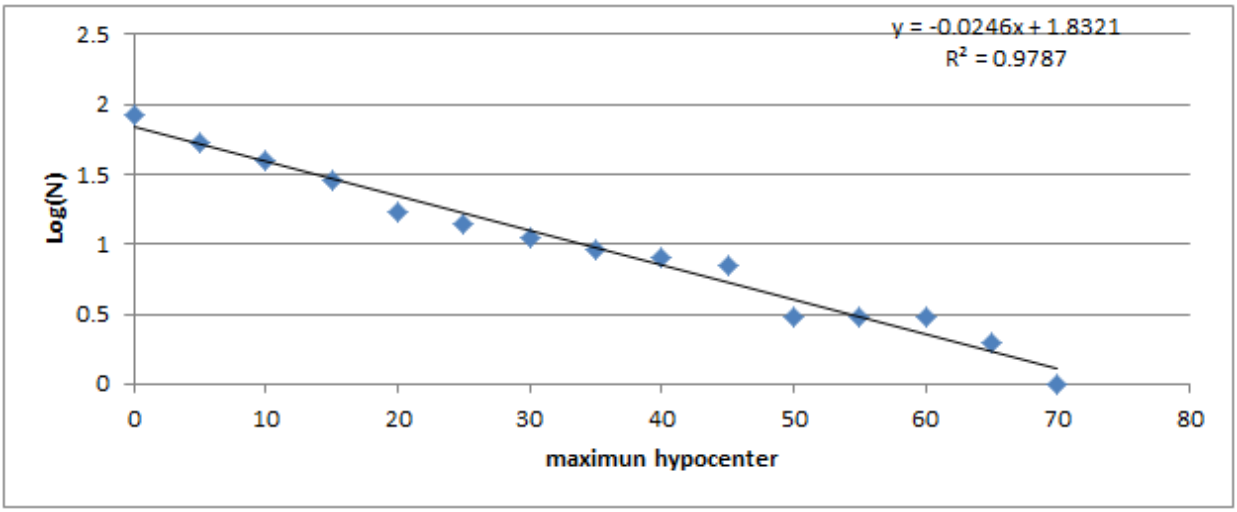

Figure 22: Modeling of the ground structure around Riragongo

This modeling shows that the number of earthquakes decreases inversely with increasing depth and that seismic activity is, on average, limited to a depth of 75 km.

The curve below depicts the DRC's seismic activity as measured by the b-value (0.9918, angular coefficient of the line).

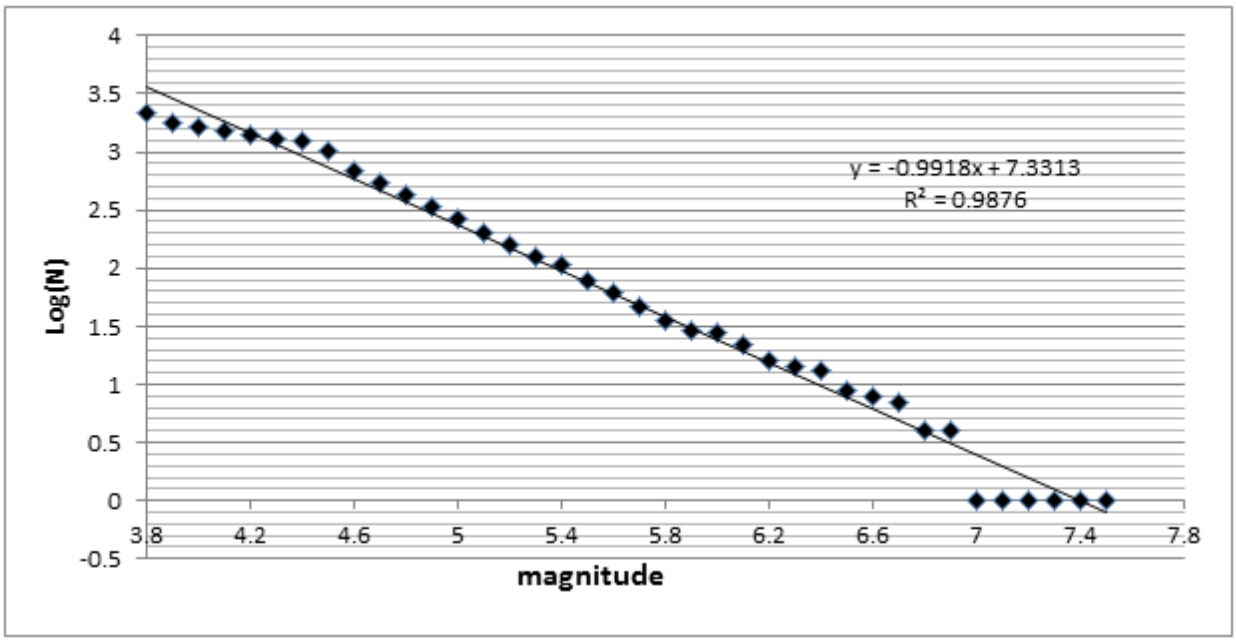

Figure 23: Seismic activity modeling in the DRC (Mukange, 2021b)

Because the two lines (Figure 22-23) have the same trend or shape, it is reasonable to conclude that there is a linear relationship between soil structure and seismic activity.

3.2.2.4.4. Distribution of seismic power and number of earthquakes by sub-area

The curve below depicts the distribution of earthquakes and power in each sub-area.

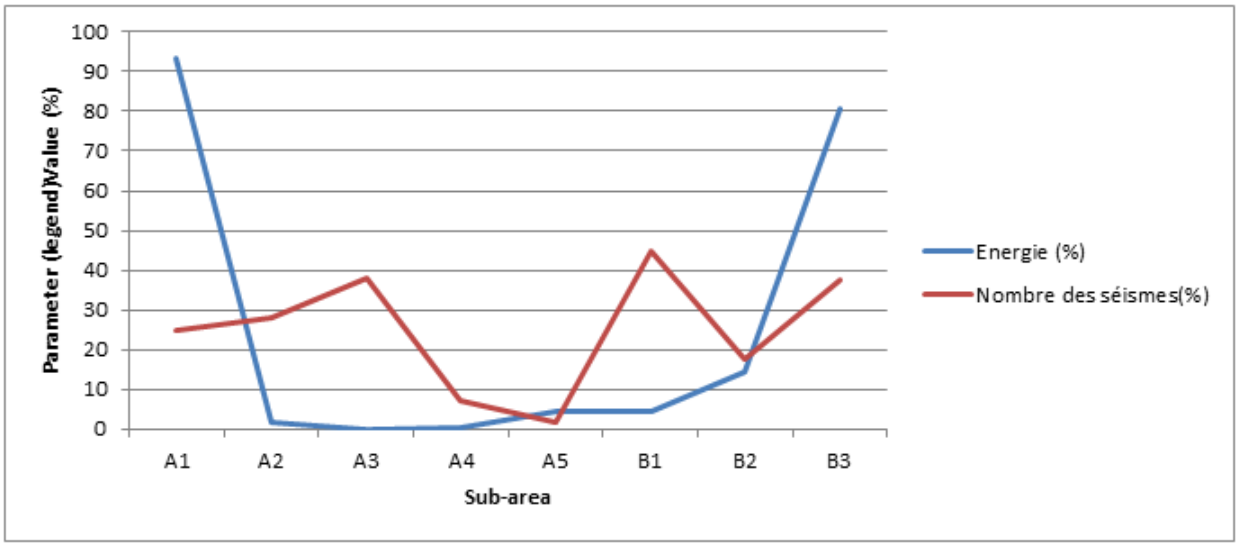

Figure 24: Distribution of seismic energy and number of earthquakes by sub-area

We can deduce the following from this graph:

- The number of earthquakes increases as Ai and Bi increase, respectively, at A3 and B1.
- According to Ai and Bi, the energy released in A1 and B3 is greater, respectively.
- The number of earthquakes is lower at A5 and B2, according to Ai and Bi.
- As a function of Ai and Bi, the energy released is lower at A3, A4, and B1.
- With some exceptions, there is a link between low energy and a low number of earthquakes.
- There is no correlation between maximum energy and the number of earthquakes, and vice versa.

The curve below depicts the distribution of earthquake density and power in each sub-area.

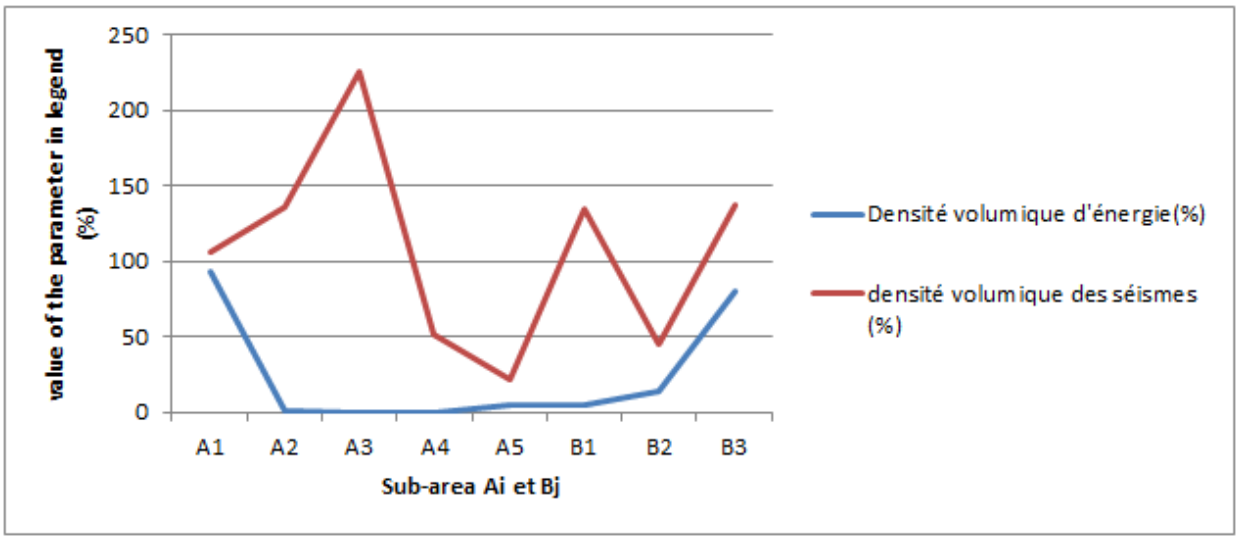

Figure 25: Distribution of seismic energy density and earthquakes by sub-area.

The figure above depicts:

- As a function of Ai and Bi, the volume density of earthquakes is higher at A3 and (B3,B1), respectively.
- As a function of Ai and Bi, the volume density of released energy is greater at A1 and B3, respectively.
- As a function of Ai and Bi, the volume density of earthquakes is lower at A5 and B2, respectively.
- As a function of Ai and Bi, the volume density of the released energy decreases at A3 and A4 and B1, respectively.
- With a few exceptions, there is a correlation between the minimum energy density and the maximum density of earthquakes at the same location, and vice versa, confirming our hypotheses.

We conclude that it is preferable to characterize seismicity in terms of volume density rather than number of earthquakes or energy. Thus, the concept of volume density is crucial in this study and in the field of characterization in general.

The legend in the figure below attempts to establish a possible correlation between the three curves.

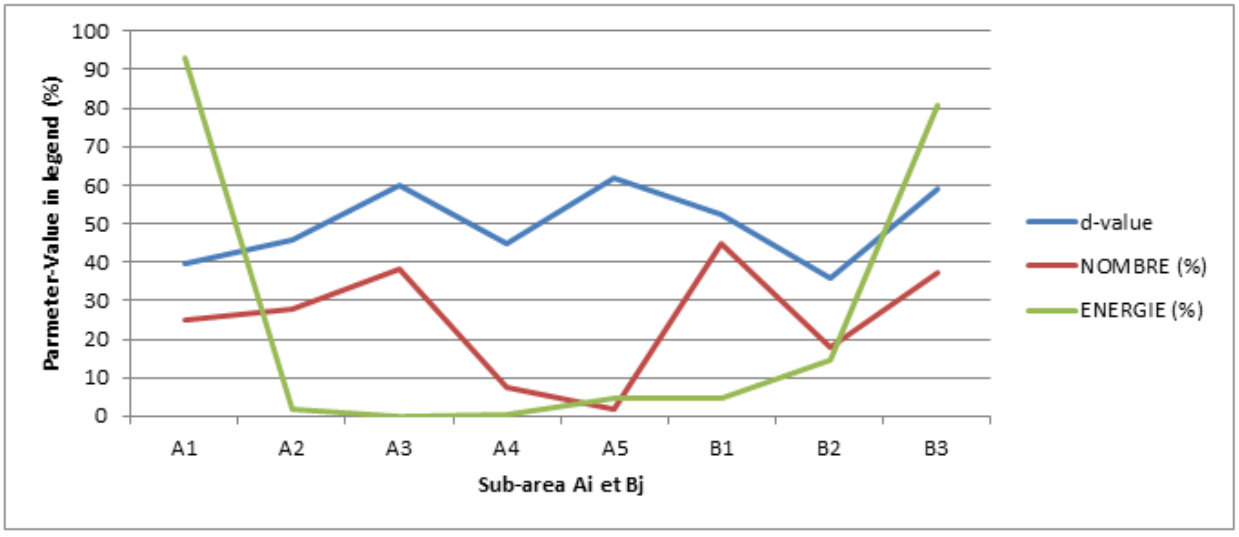

Figure 26: Distribution of power, number of earthquakes, and d-value by sub-zone.
NB: the d-value has been multiplied by 2000.

Once again, there is a strong correlation between the number of earthquakes curve and the d-value (which characterizes the structure of the ground). We conclude and confirm that seismic activity is influenced by ground structure.

3.2.3. Division of the area into grid-areas (cij)

The concept of grid-areas is similar to the concept of vector representation (Mukange, 2021a-b).
Indeed, the grid-zone Cij is formed by the intersection of the sub-areas Ai and Bj.
As a result, cij is described as follows:

The seismic level values (a i) of the vertical sub-areas (Ai) are taken by I and the seismic level values (b j) of the horizontal sub-areas are taken by j. (Bj).

We can calculate the module of the subzones cij using the relation

$$c = \sqrt{a_i^2 + b_j^2} \qquad (12).$$

In accordance with the code of table (9), we assign a color to each modulus (Table 10).

Table 9 : shows the color code for the module slice.

MODULE	Level	Colours
$[1,2]$	1	Pink
$]3,4]$	2	Light blue
$]5,6]$	3	Purple
$]7,8]$	4	Green
$]9,10]$	5	Yellow
$]11,12]$	6	Orange
$]13,14]$	7	Light red

Table 10: Assignment of color to the module of each zone-grid cij

AREAS-GRIDS	b	a	MODULE	SEISMIC LEVEL	COLOUR CODE
C11	6	7	9,21	5	Yellow
C12	6	4	7,21	4	Purple
C13	6	5	7,81	4	Purple
C14	6	3	6,7	4	Purple
C15	6	2	6,32	4	Purple
C21	1	7	7,07	4	Purple
C22	1	4	4,12	3	Green
C23	1	5	5,09	3	Green
C24	1	3	3,16	2	Light blue
C25	1	2	2,23	2	Light blue
C31		7	10,63	6	Orange
C32	8	4	8,94	5	Yellow
C33	8	5	9,43	5	Yellow
C34	8	3	8,54	5	Yellow
C35	8	2	8,24	5	Yellow

The results of the above table, particularly the use of the color code, lead to the characterization of grid-areas in the form of seismic zoning (Figure 27), highlighting five groups:

Table 11: Color statistics (module)

N°	COLOURS	AREAS-GRIDS	CONTRIBUTION(%)
1	PURPLE	C12, C13, C14, C15, C21	5/15 (33%)
2	BLUE	C24, C25	2/15 (13,3%)
3	GREEN	C22, C23	2/15(13,3%)
4	YELLOW	C11, C32, C33, C34, C35	5/15 (33%)
5	ORANGE	C31	1/15 (7%)

The results of this table are converted into curves (Figure 27)

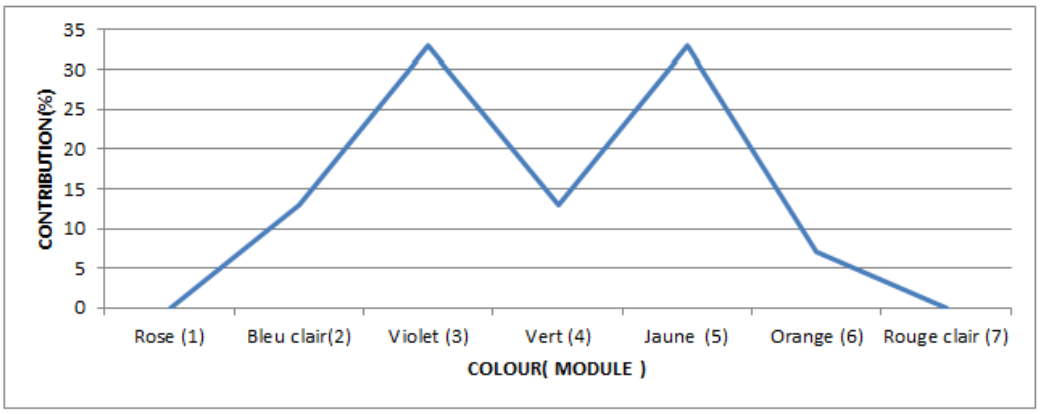

Figure 27: Color distribution (module) in Nyiragongo grid areas.

We estimate the degree of homogeneity at 33% (5 groups out of 15 Cij), corresponding to a degree of heterogeneity of 67%.

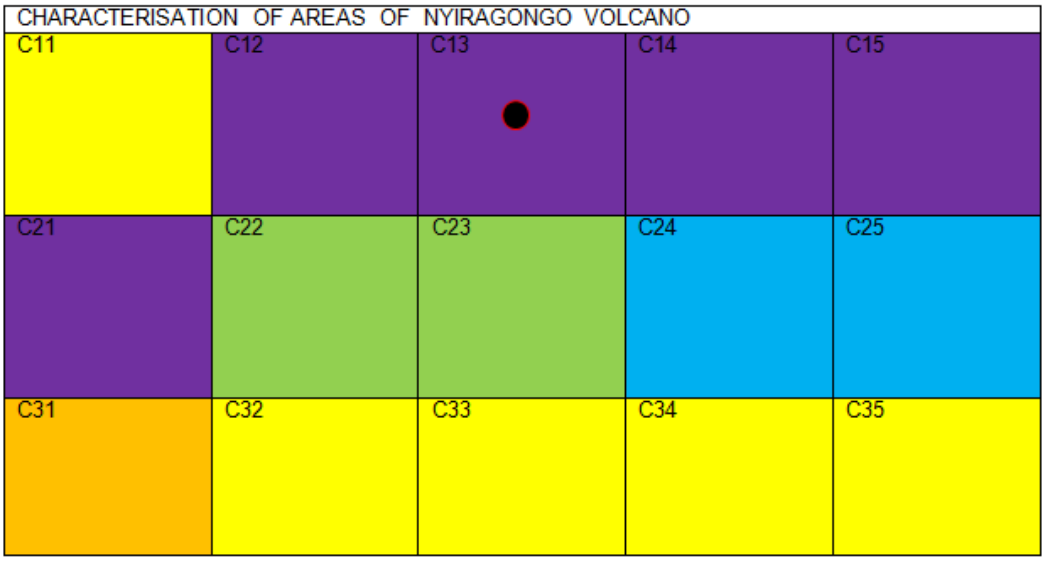

Figure 28: Characterization of seismic activity using the zoning map of areas

The results of the table are transformed into curves (Figure 29) and show the following:

- Seismic activity decreases from west (A1) to east (A5), - The B1 sub-area is the transition zone between B2 (low activity) and B3 (high activity) (high seismic activity).

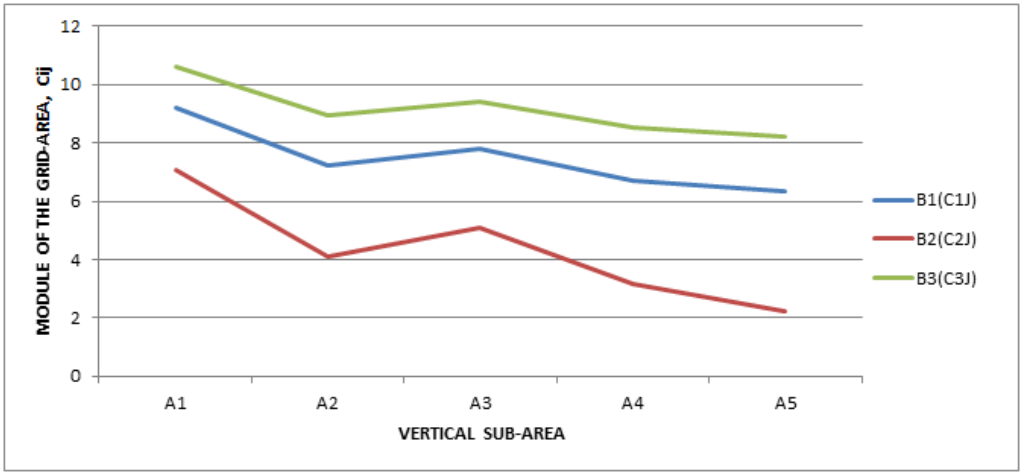

Figure 29 : Figure 29: Characterization of seismicity by using the curves

Finally, the degree of heterogeneity is calculated as follows: - For horizontal sub-areas (Bj), we calculate the percentage of the number of different colors recorded to the total number of Cij (five for each Bj).

- For the vertical sub-areas (Ai), we calculate the percentage of the number of different colors recorded to the total number of Cij (three for each Ai).
- The final degree of homogeneity is simply the mean of these two (Ai and Bj) (Table 12)
- At the level of sub-areas A4 and A5, an anomaly appears: the gap between the blue and red curves becomes extremely large (Figure 29).

Table 12: degree of heterogeneity relative to each sub-area

Sub-areas	Degree of heterogeneity	Degree of heterogeneity in %
B_1	3/5	60 %
B_2	4/5	80 %
B_3	3/5	60 %
A_1	3/3	100 %
A_2	3/3	100 %
A_3	3/3	100 %
A_4	3/3	100 %
A_5	3/3	100 %
Average		700/800 =88%

The degree of heterogeneity has increased from zero to 88%.
According to the formula, the rate of heterogeneity é is 56% (5/9) when the number of distinct colors (5) in the figure (28) is divided by the total number of colors in the table (9)

When the number of distinct colors (5) in the figure (28) is divided by the total number of boxes (15) in the figure (28), the rate of heterogeneity é is calculated to be 33% (5/15). We'll stick with the first formula.

3.2.4 Comparison of the structural curves

To compare three structural curves obtained through various studies, we present them below.

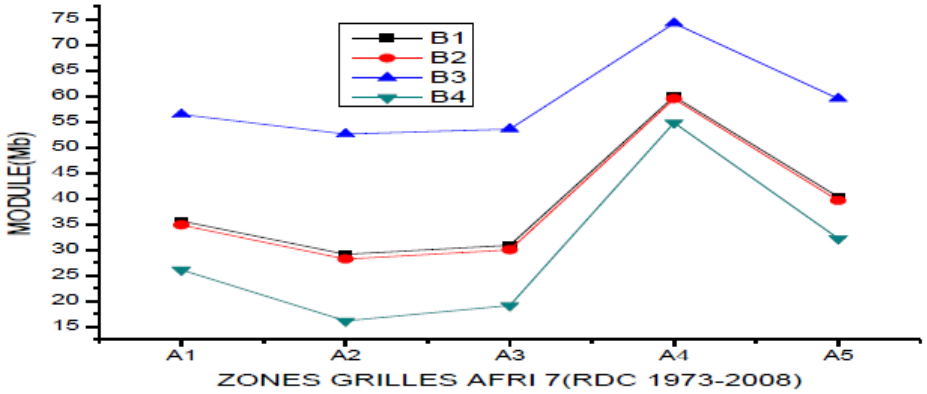

Figure 30: Structural curve of the DRC (10°E-35°E; 6°N-14°S), (Mukange,2021b)

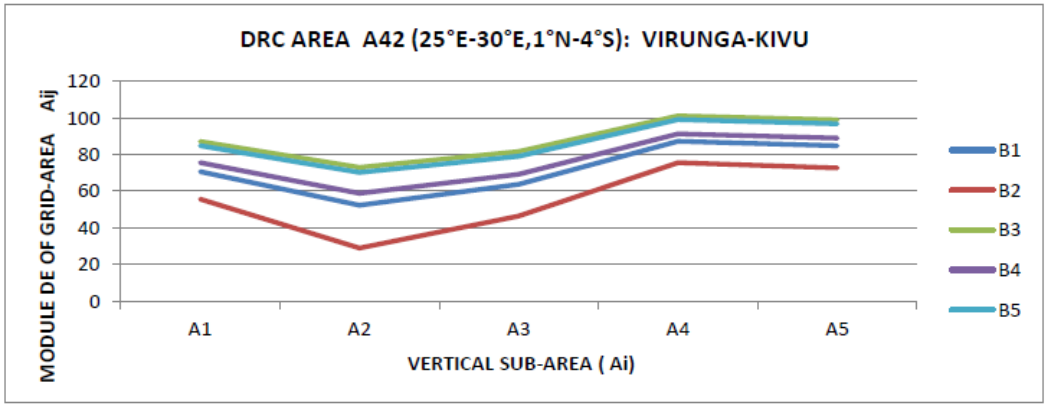

Figure 31: Structural curve of the Virunga area (25°E-30°E; 1°N-4°S),(Mukange,2022a)

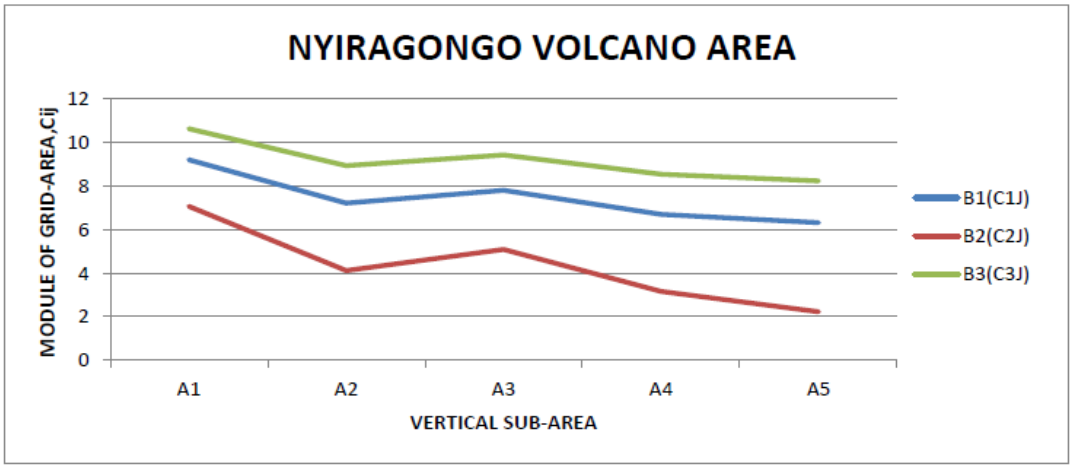

Figure 32: Structural curve of Nyiragongo Volcano area (29.0°E-29.5°E; 1.45°S-1.75°S)

Analysis of these three structures reveals the following:

- Moving from west to east (Ai), the shape is the same for the DRC (Figure 30) and the Virunga region (Figure 31); they are the inverse of Nyiragongo (Figure 321). This difference is due to the fact that the Nyiragongo zone is located in the front (29°E), a less seismic area , whereas the area of major fractures and intense seismic activity is located between 30°E and 35°E.
- From North to South (Bj), the three structures exhibit the same trend: seismic activity decreases from north to south.
- These findings support previous research (Mukange, 2016), which found that the DRC's seismicity is better described (diversified) in terms of longitude (West to East) than latitude (North to South).

3.2.5. Crater location

Starting with the assumption that the crater is located where: - the volume density of the number is abnormally high, - the volume density of the seismic energy of tectonic or volcano-tectonic earthquakes is very low.
Based on these assumptions, other distinguishing features, and the application of the results in Figures (24-25), the crater of Nyiragongo volcano is located at subarea C13 (B1, A3) [29.25°E; 1.50° S]. The black bubble in Figure indicates this location (28). These findings are consistent with the observations made in the field (Figure 5). This confirms our hypotheses, which should be generalized and confirmed through additional research.

4. GENERAL CONCLUSION AND PERSPECTIVES

The design of a characterization scale enabled the study of volcano-seismic activity in the vicinity of the Nyiragongo volcano in the DRC's Virunga area, the western branch of the East African Rifts, as well as the search for techniques for locating its crater on the basis of seismic data. This scale,,, very simplified because it contains only three parameters, introducing the structure constant known as the d-value and the concept of the volume density of energy or number of earthquakes has produced the following results:

- This once homogeneous area, now subdivided into sub-areas, is no longer homogeneous: When examined vertically and horizontally, it reveals a degree of heterogeneity of 80 and 100%, respectively.
- The final degree of heterogeneity of the area is 88%, ranging from homogeneous to 12%. Thus, a structure's homogeneity is determined by the scale used to observe it.
- The seismic species identified in this area are Iab, Iac, Ibb, Ibc, IIIbb, and IIIbc, while the structure factors are (ab, ac, bb and bc).
- Analysis of these three structures, DRC (10°E-35°E; 6°N-14°S), Virunga area (25°E-30°E; 1°N-4°S°), and around Nyiragongo Volcano (29.00°E-29.50°E; 1.45°S-1.75°S), reveals the following:

Going from West to East (Ai), the shape of structures is the same for the Democratic Republic of Congo and Virunga; they are opposites of Nyiragongo. This difference is due to the fact that the Nyiragongo zone is located before (29°E), a less seismic area, whereas the area of major fractures and intense seismic activity is located between 30°E and 35°E. Around 28°E, Virunga and Nyiragongo structures share the same shape. From North to South (Bj), the three structures follow the same pattern: Seismic activity decreases from North to South.

These findings support previous research (Mukange, 2016), which found that the seismicity of the Democratic Republic of Congo is better described (diversified) in terms of longitude (West to East) than latitude (North to South).

- The ground structure surrounding the volcano from North to South (horizontal subdivision) is similar to that studied in the Virunga region at a depth ranging from 25 to 105 km; - the soil structure surrounding Nyiragongo volcano

following vertical subdivision (Ai) is similar to that studied in the Virunga area's granitic area.
- We see a strong correlation between the number of earthquakes and the d-value once more (characterizes the ground structure). We conclude and confirm that seismic activity is determined by the ground structure. - In a volcanic area, there is a correlation between the maximum volume density of tectonic earthquake energy and the minimum density of earthquakes, with some nuances.
- It is preferable to characterize seismicity in terms of volume density rather than number of earthquakes or energy. Volume is thus an important concept in this study.
- The confirmation of the crater's location assumptions Indeed, these are the assumptions:

The crater is located in an area with an abnormally high volume density of volcanic earthquakes. - Using these assumptions and other distinguishing factors, we were able to pinpoint the crater of Nyiragongo volcano at [29.25°E; 1.50°S]. These findings are consistent with field observations. Nonetheless, confirmation of these hypotheses is required before they can be generalized. As a result, we must continue our research using our model.

REFERENCES

1. Bahaya B., (2021). *Modélisation numérique du transfert de chaleur par conduction au sein du volcan Nyiragongo.* Thèse de Doctorat : Université Pédagogique Nationale, Faculté des Sciences. Département de Physique

2. Bantidi M., Wafula M., Mavambou, Mukange B., Zana Nd., (2014a). Probabilistic assessment of seismic hazard in Lake Tanganyika Rift accounting for local geologies conditions. 2015. *International Journal of Geology, Agriculture and Environmental Sciences*. Vol.03 Issue 02 (April 2015), pp24-29.

3. Bantidi M., Mukange B., et Zana N., (2014b). Structure de la sismicité de la Branche occidentale des Rifts Valleys du système des Rifts Est-africains ; de 1954 à 2010, *International Journal of Innovation and Applied Studies*, ISSN 2028-9324 Vol. 9 No. 4 Dec. 2014, pp.1562-1581.

4. Borden J-P., (1988). *Biologie-Géologie*. Première S. Paris: Bordas

5. Kamate K., (2018). *Pétrographie et géochimie des laves du volcan Nyiragongo (Nord Kivu, RD Congo) : influence de la viscosité sur les paramètres de propagation des coulées de laves menaçant la ville de Goma*. Master de spécialisation : Université de Liège, Faculté des Sciences. Département des Sciences et Gestion de l'Environnement. http://hdl.handle.net/2268.2/5534

6. Lay T., Wallace T., (1995). *Modern Global seismology*. New-York : Academic Press

7. Lubemba A., (2021). *Analyse des effets des gaz volcaniques et des ilots d'évapotranspiration sur les paramètres climatiques autour du Volcan*. Thèse de Doctorat : Université Pédagogique Nationale, Faculté des Sciences. Département de Physique

8. Mukange B., Bantidi M., Zana Nd. (2013). Structure de la sismicité de la Branche orientale des Rifts Valleys du système des Rifts Est-africains ; de 1954 à 2010. *Revue Congolaise des Sciences Nucléaires.* vol.27, pp 151-169.

9. Mukange B., Bantidi M., Zana L., Wafula M., Zana Nd. (2015). The isoseismal map and their implication to underlining ground degree of heterogeneity (Kabalo quake's case, September 11, 1992, magnitude 6.7, Upemba Rift). *Greener Journal of Geology and Earth Sciences*, vol. 3 (2), pp 030-042.

10. Mukange B., (2016). *Conception d'un modèle physique pour la caractérisation et la surveillance de l'activité sismique et son implication géologique (Cas de la République Démocratique du Congo).* Thèse de Doctorat : Université de Kinshasa, Faculté des Sciences. Département de Physique.

11. Mukange Besa, (2021). *Cours de Géophysique générale*. Université de Kinshasa, Faculté des Sciences.

12. Mukange B., (2021a). Design of a unified scale for the characterization of seismic activity. International Journal of Innovative Science and Research Technology, Volume 6, Issue 7, July– 2021, pp.1407-1422. www.ijisrt.com

13. Mukange B., (2021b). Application of the unified scale to the characterization of seismic activity of the Democratic Republic of Congo and its surroundings (comparative study for Africa, Indonesia and the Pacific coast of Central America). International Journal of Innovative Science and Research Technology, Volume 6, Issue 7, July– 2021, pp.1516-1555. www.ijisrt.com

14. Mukange B., (2023b). Characterization of the volcano-seismic activity around Nyamulagira volcano and location of its crater by means of unified scale. *Greener Journal of Geology and Earth Sciences*, 5(1) December 2023: 52-75. http//gjournals.org/GJGES.

15. Mukange B., (2023c). Highlighting the fine structure of the seismic zones of the western branch of the east african rift system using the unified characterization scale and its geological implication . *Greener Journal of Geology and Earth Sciences*, 5(1) December 2023: 76-108. http//gjournals.org/GJGES.

16. Ongendangenda A., (2020). Volcanologie de la chaîne des Virunga. Paris: L'Harmattan.

17. Wafula M., D. Atiamutu et M. Ciraba, (1999). Activité séismique dans les Virunga (Rép.Dém. Congo) liée aux éruptions du Nyiragongo et Nyamuragira, deNovembre 1994 à Décembre 1996. *Mus. roy. Afr. centr. Tervuren Belg., Dépt. Géol. Min. Rapp. Ann. 1997 & 1998*, pp. 309 - 319.

18. Wafula M.D., Kasereka M., Rusangiza K., Kuvuke K., Mukambilwa K., Ciraba M. &Bagalwa M., (2009). The Nyamulagira Volcanic Eruption on November 27, 2006, Virunga Region, D.R. Congo. *Cahiers du CERUKI, Numéro Spécial CRSN-Lwiro(2009)*, pp. 108 - 115.

19. Wafula M.D, Zana A. Kasereka M. and Hamaguchi H., (2011a). The Nyiragongo volcano: A case study for the Mitigation of Hazards on an African Rift Volcano, Virungaregion, Western African Rift Valley, 32 pp.
Disponible sur: *http://iugg georisk.org/presentations*

20. Wafula M., (2011b). *Etude Géophysique de l'Activité Volcano-Séismique de la Région des Virunga, Branche Occidentale du Système des Rifts Est-Africains et son Implication dans la Prédiction des Eruptions Volcaniques*. Thèse de Doctorat : Université de Kinshasa, Faculté des Sciences.

21. Zana N, (1977). *The Seismicity of the Western Rift Valley of Africa and related problems.* Doctorat Theses, Tôhoku University. 189 pp.

22. Zana N. and K. Tanaka, (1981). Focal mechanism of major earthquakes in the WesternRift Valley of Africa, *Tôhoku Geophys. Journ. (Sci. Rep. Tôhoku Univ. Ser. 5),* Vol.28, Nos 3-4, pp: 119 - 129.

23. Zana Ndontoni A., (2004), Cours de Géophysique : Introduction à la géophysique générale, UNIKIN, Kinshasa

24. Zana A., (2010), Détonateur Potentiel de Tsunami au lac Kivu, Conférence débat,

Cite this Article: Mukange, BA; Ntedika, ME; Zana, NA; Tondozi, KF (2023). Characterization of the Volcano-Seismic Activity around Nyiragongo Volcano and Location of its Crater by Means of Unified Scale. *Greener Journal of Geology and Earth Sciences*, 5(1): 28-51.